Video Article

Integrated Photoacoustic Ophthalmoscopy and Spectral-domain Optical Coherence Tomography

Wei Song*[1,2], Qing Wei*[1], Shuliang Jiao[3], Hao F. Zhang[1,4]

[1]Department of Biomedical Engineering, Northwestern University

[2]Department of Physics, Harbin Institute of Technology

[3]Department of Ophthalmology, University of Southern California

[4]Department of Ophthalmology, Northwestern University

*These authors contributed equally

Correspondence to: Hao F. Zhang at hfzhang@northwestern.edu

URL: https://www.jove.com/video/4390
DOI: doi:10.3791/4390

Keywords: Biomedical Engineering, Issue 71, Bioengineering, Medicine, Anatomy, Physiology, Opthalmology, Physics, Biophysics, Photoacoustic ophthalmology, ophthalmoscopy, optical coherence tomography, retinal imaging, spectral-domain, tomography, rat, animal model, imaging

Date Published: 1/15/2013

Citation: Song, W., Wei, Q., Jiao, S., Zhang, H.F. Integrated Photoacoustic Ophthalmoscopy and Spectral-domain Optical Coherence Tomography. *J. Vis. Exp.* (71), e4390, doi:10.3791/4390 (2013).

Abstract

Both the clinical diagnosis and fundamental investigation of major ocular diseases greatly benefit from various non-invasive ophthalmic imaging technologies. Existing retinal imaging modalities, such as fundus photography[1], confocal scanning laser ophthalmoscopy (cSLO)[2], and optical coherence tomography (OCT)[3], have significant contributions in monitoring disease onsets and progressions, and developing new therapeutic strategies. However, they predominantly rely on the back-reflected photons from the retina. As a consequence, the optical absorption properties of the retina, which are usually strongly associated with retinal pathophysiology status, are inaccessible by the traditional imaging technologies.

Photoacoustic ophthalmoscopy (PAOM) is an emerging retinal imaging modality that permits the detection of the optical absorption contrasts in the eye with a high sensitivity[4-7] . In PAOM nanosecond laser pulses are delivered through the pupil and scanned across the posterior eye to induce photoacoustic (PA) signals, which are detected by an unfocused ultrasonic transducer attached to the eyelid. Because of the strong optical absorption of hemoglobin and melanin, PAOM is capable of non-invasively imaging the retinal and choroidal vasculatures, and the retinal pigment epithelium (RPE) melanin at high contrasts [6,7]. More importantly, based on the well-developed spectroscopic photoacoustic imaging[5,8] , PAOM has the potential to map the hemoglobin oxygen saturation in retinal vessels, which can be critical in studying the physiology and pathology of several blinding diseases [9] such as diabetic retinopathy and neovascular age-related macular degeneration.

Moreover, being the only existing optical-absorption-based ophthalmic imaging modality, PAOM can be integrated with well-established clinical ophthalmic imaging techniques to achieve more comprehensive anatomic and functional evaluations of the eye based on multiple optical contrasts[6,10] . In this work, we integrate PAOM and spectral-domain OCT (SD-OCT) for simultaneously *in vivo* retinal imaging of rat, where both optical absorption and scattering properties of the retina are revealed. The system configuration, system alignment and imaging acquisition are presented.

Video Link

The video component of this article can be found at https://www.jove.com/video/4390/

Protocol

1. System Configuration

1. *PAOM Subsystem*
    1. Illumination source: a Nd:YAG laser (SPOT-10-100, Elforlight Ltd, UK: 20 μJ/pulse; 2 nsec pulse duration; 30 kHz maximum pulse repetition rate).
    2. The output laser at 1064 nm is frequency-doubled to 532 nm by a beta-barium-borate (BBO) crystal (CasTech, San Jose, CA). After further split by a laser line mirror, 532 nm light is delivered through a single-mode optical fiber (P1-460A-FC-5, Thorlabs), and 1064 nm laser is recorded by a photodiode (DET10A, Thorlabs), which triggers PA signal acquisition.
    3. The laser light coming out of the single-mode optical fiber is delivered onto the retina by a galvanometer (GM, QS-7, Nutfield Technology) and a telescope configuration (f1=75 mm and f2=14 mm, Edmund Optics)[6].
    4. An unfocused needle transducer (40-MHz central frequency, 16-MHz bandwidth, 0.4×0.4 mm^2 active element size, NIH Resource Center for Ultrasonic Transducer Technologies, The University of Southern California) is placed in contact with the eyelid to detect

the PA signals generated from the retina. Ultrasonic gel (Sonotech) is applied between the transducer tip and animal eyelid for good acoustic coupling.
5. The PA signal is amplified by two amplifiers (ZFL-500LN+, Mini-circuits, and 5073PR, Olympus), and is digitized by a data acquisition board (CS14200, Gage Applied).

2. *SD-OCT Subsystem*
   1. Low coherence light source: a broadband super-luminescent diode (IPSDD0804, InPhenix; center wavelength: 840 nm; 6-dB bandwidth: 50 nm), which determines the axial resolution of 6 μm.
   2. The near infrared light is split to reference arm and sample arm by a 50×50 customized single-mode fiber coupler (OZ Optics).
   3. After combining with PAOM illuminating light by a hot mirror (FM02, Thorlabs), OCT sample arm shares the same scanning and delivery optics with PAOM[6].
   4. A home-built spectrometer is used to record the SD-OCT interference signals, where a line scan CCD camera (Aviiva SM2, e2v) allows an A-line rate of 24 kHz. Design of typical spectrometers can be found from several previously published literatures[11]and fiber-coupled SD-OCT spectrometers are now commercially available. The SD-OCT sensitivity is measured to be better than 90 dB.

3. *Scanning Scheme*
   1. Fast 2-D raster scanning of the galvanometer is controlled by an analogue output board (PCI-6731, National Instruments), which also triggers both the PAOM laser firing and the signal acquisition of OCT spectrometer. As a result, the data acquisitions in PAOM and OCT subsystems are synchronized.
   2. The PAOM data acquisition is triggered by a photodiode recording PAOM laser sequence (see 1.1.2).
   3. 3-D volumetric images or 2-D fundus images are constructed from 256 B-scan images (256 A-lines per B-scan image).

2. System Alignment

1. Maximize the frequency-doubling efficiency of the BBO crystal and the coupling efficiency of the single-mode optical fiber. Wear LG3 goggles (Thorlabs) for personnel eye protection when optimizing the PAOM illuminating light.
2. Collimate the fiber output laser of PAOM to 2.0 mm in diameter.
3. Align the combined illumination lights of PAOM and SD-OCT to be coaxial.
4. Set the PAOM excitation light at ~40 nJ/pulse and SD-OCT probing light at ~0.8 mW, both of which are reported to be eye safe [6,12].

3. *In vivo* Multimodal Retinal Imaging

1. Transfer the rat to a transparent polypropylene box, and anesthetize the animal by a mixture of isoflurane (Phoenix pharmaceutical, Inc.) and normal air at a concentration of 1.5% and a flow rate of 2.0 liter/min for 10 min.
2. Restrain the anesthetized rat in a homemade holder with five-axis adjustable freedom (**Figure 1**), and keep its body temperature at ~37 °C by a heating pad (Repti therm, Zoomed laboratories, Inc.). Maintain the anesthesia by inhalation gas of mixed isoflurane and normal air with 1.0% concentration and 1.5 liter/min flow rate throughout the experiment.
3. Cut the eyelash using a surgical scissors, dilate the pupils with 1% Tropicamide ophthalmic solution, and paralyze the iris sphincter muscle using 0.5% Tetracaine Hydrochloride ophthalmic solution. Apply artificial tear drops (Systane, Alcon Laboratories, Inc.) to the rat eye every other minute to prevent cornea dehydration and cataract formation. Monitor the animal heart rate, respiration, and blood oxygenation by a pulse oximeter (8,600 V, Nonin Medical, MN) during imaging.
4. Turn on SD-OCT illuminating light and check the probing light to be ~0.8 mW.
5. Activate the galvanometer scanning. Align the SD-OCT irradiation light delivery onto the rat retina and identify the retinal region of interest (ROI) by adjusting the five-axis animal holder. Here, the optic disc is intentionally placed in the center of the field of view, while the ROI should be selected based on different research requirements.
6. Further adjust the animal holder to optimize the SD-OCT imaging qualities of retinal cross section in both scanning directions (by switching the raster scanning direction) until the best optical focus is reached.
7. Prepare the needle transducer on a five-axis adjustable platform, apply a drop of ultrasonic gel to the transducer tip, and gently contact the transducer tip to the animal eyelid.
8. Set PAOM laser to the external-trigger mode, start the galvanometer scanning, and activate real-time display of PAOM cross-sectional image of the animal retina. Carefully adjust the transducer orientation until the PAOM image has the best signal-to-noise ratio (SNR) and, in the meantime, shows an evenly distributed PA amplitude patterns in both scanning directions.
9. Set the scanning parameters, and conduct the simultaneous retinal imaging of SD-OCT and PAOM. Reconstruct the three-dimensional images of SD-OCT and PAOM off-line. Our reconstruction codes were written in Matlab and three-dimensional visualization was achieved uing a freeware (Volview, Kitware). The algorithm for SD-OCT reconstruction can be found in Ref. [11] and the algorithm for PAOM reconstruction can be found in Ref. [6] and Ref.[13]. If needed, repeat procedures of 3.7)-3.9).
10. After experiment, turn off the SD-OCT probing light, remove the animal from holder immediately, and keep it warm until it wakes up naturally. Keep the animal in a dark environment for an extra hour for eyes to recover. The whole experimental duration, including the animal anesthesia and imaging acquisition, is less than 30 min for an experienced operator.

Representative Results

Figure 2 shows the 2-D fundus images of SD-OCT and PAOM acquired simultaneously in an albino rat (**A and B**) and a pigmented rat (**C and D**), respectively. In the SD-OCT fundus images (**Figures 2A and 2C**), retinal vessels have dark appearance due to the hemoglobin absorption of probing light. In addition to retinal vessels (**RV in Figure 2B**), PAOM visualizes the choroidal vasculatures (**CV in Figure 2B**) in albino eye because of the lacking RPE melanin. Because pigmented eye has high melanin concentration, PAOM images RPE (**Figure 2D**) with high contrast in addition to the retinal vessels. In all retinal imaging, the maximum scanning angle is 26 degrees and the imaging acquisition takes

~2.7 sec. To demonstrate the three-dimensional imaging capability of PAOM, a volumetric rendering of the data shown in **Figure 2b** is given in **Figure 3**.

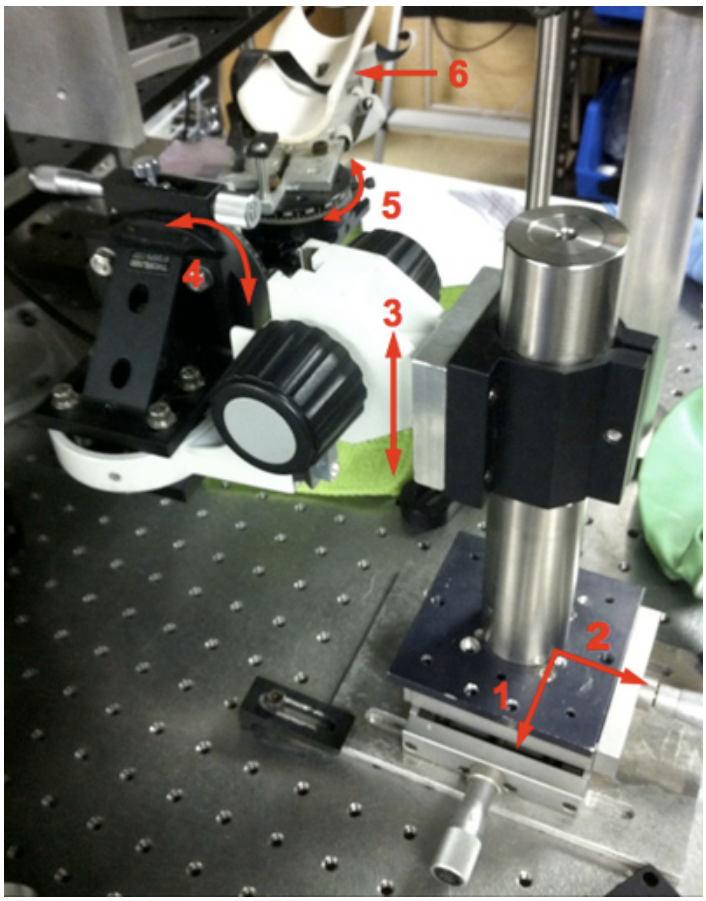

Figure 1. Photograph of the five-axis animal holder. The arrows 1-5 highlight the five adjustable freedoms and the arrow 6 highlights the animal restrainer.

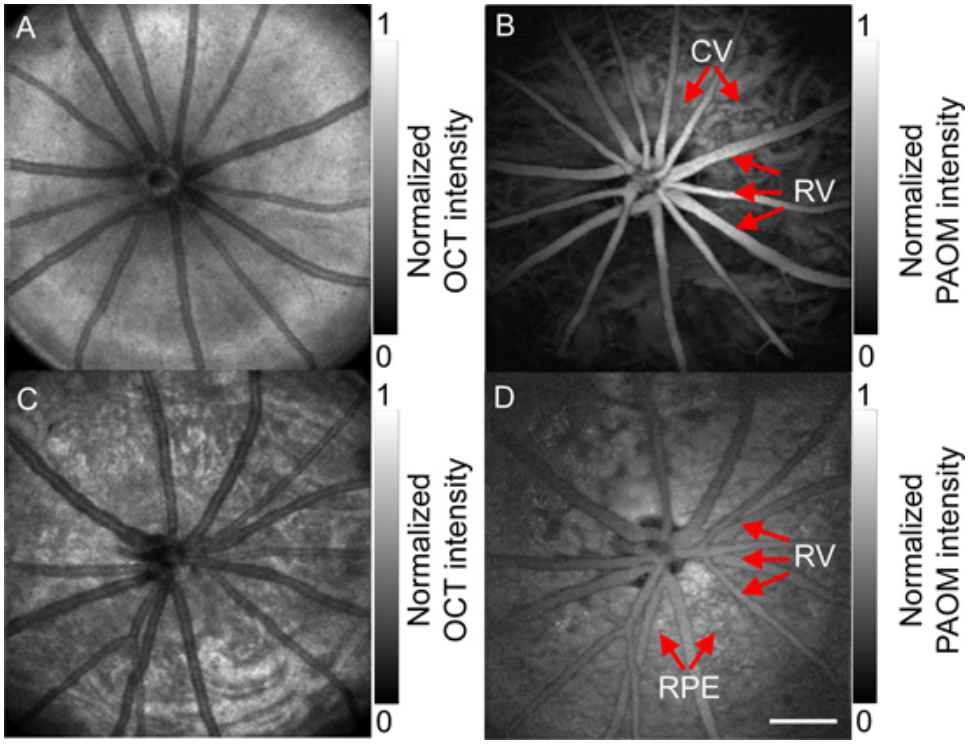

Figure 2. Simultaneously acquired SD-OCT (A and C) and PAOM (B and D) fundus images. A) and B) are acquired from an albino rat, and C) and D) are acquired from a pigmented rat. RV: retinal vessel; CV: choroidal vessel; RPE: retinal pigment epithelium. Bar: 500 μm.

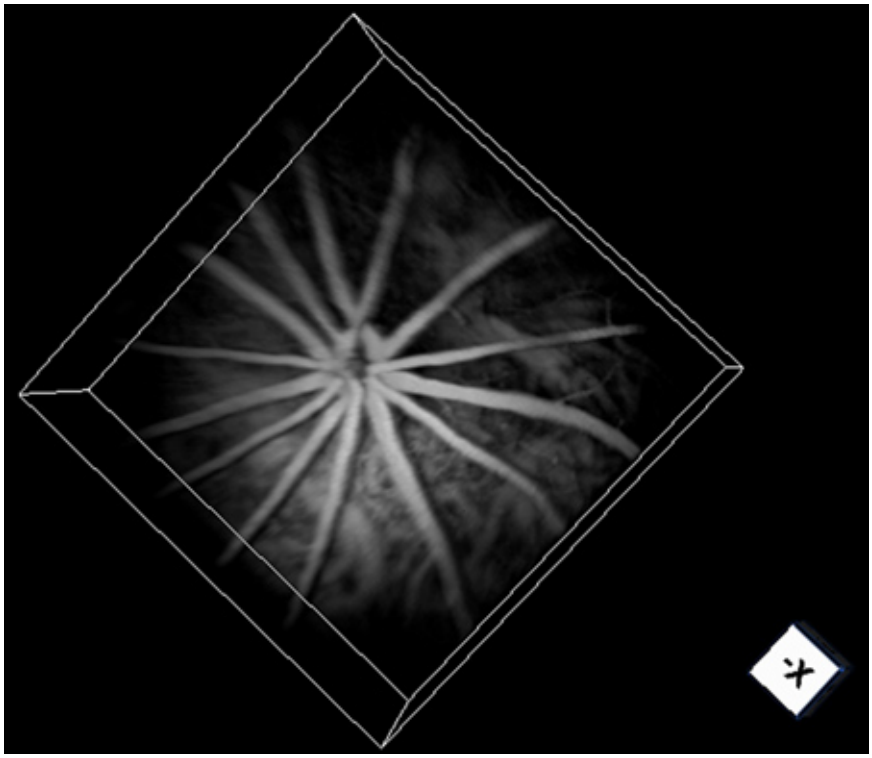

Figure 3. Volumetric visualization of PAOM in an albino rat retina.

Discussion

Here, we present a detailed instruction on simultaneous *in vivo* retinal imaging of rat eyes using PAOM combined with SD-OCT. Optical-scattering-based SD-OCT is, perhaps, the clinical "gold standard" for retinal imaging[3]; however, it is not sensitive to detect the optical absorption in the retina. The newly-developed PAOM is the only optical-absorption-based ophthalmic imaging modality that provides optical

absorption properties of the retina[6]. Because hemoglobin and melanin are endogenously strong optical absorbing pigments, PAOM enables the investigating of the anatomy and functions of the retinal/choroidal vessels and the RPE without resorting to additional contrast agents.

In PAOM, the unfocused ultrasonic transducer has a limited sensitivity region (~2.8×2.8 mm^2)[10] due to its finite active element, which causes a decayed detection sensitivity of PA signals toward the periphery of the field of view (FOV). Thus, the tilting angle of the transducer should be carefully adjusted to achieve a homogeneous retinal FOV. A potential substitution for the traditional piezoelectric transducer is to apply micro-ring resonator, which has lower noise equivalent pressure values and wider detection directivity [14], which may provide a more homogeneous retinal image with better SNR in PAOM. Comparing with SD-OCT, PAOM has similar lateral resolution (~20 μm) but much worse axial resolution (~23 μm) due to the currently limited ultrasonic bandwidth[6]. The axial resolution of PAOM can potentially be improved by employing novel ultrasonic detector as well. The calibration method of PAOM resolutions was previous reported [6,15].

In summary, the integrated PAOM and SD-OCT imaging system offers more comprehensive anatomical and functional evaluation of the retina, and, therefore, holds great promises in the future clinical diagnosis and managements of many ocular disorders.

Disclosures

All experimental animal procedures were approved by the Institutional Animal Care and Use Committee of Northwestern University.

Acknowledgements

We thank the generous support from the National Science Foundation (CAREER CBET-1055379) and the National Institutes of Health (1RC4EY021357, 1R01EY019951). We also acknowledge the support from the China Scholarship Council to Wei Song.

References

1. Kinyoun, J.L., Martin, D.C., Fujimoto, W.Y., & Leonetti, D.L. Ophthalmoscopy versus fundus photographs for detecting and grading diabetic retinopathy. *Invest. Ophthalmol. Vis. Sci.* **33** (6), 1888-1893 (1992).
2. Schuman, J.S., Wollstein, G., Farra, T., Hertzmark, E., Aydin, A., Fujimoto, J.G., & Paunescu, L.A. Comparison of optic nerve head measurements obtained by optical coherence tomography and confocal scanning laser ophthalmoscopy. *Am. J. Ophthalmol.* **135** (4), 504-512 (2003).
3. Strøm, C., Sander, B., Larsen, N., Larsen, M., & Lund-Andersen, H. Diabetic macular edema assessed with optical coherence tomography and stereo fundus photography. *Invest. Ophthalmol. Vis. Sci.* **43** (1), 241-245 (2002).
4. Hu, S., Maslov, K., & Wang, L.V. Three-dimensional Optical-resolution Photoacoustic Microscopy. *J. Vis. Exp.* (51), doi:10.3791/2729 (2011).
5. Wang, L.V. Multiscale photoacoustic microscopy and computed tomography. *Nat. Photonics.* **3** (9), 503-509, doi:10.1038/Nphoton.2009.157 (2009).
6. Jiao, S., Jiang, M., Hu, J., Fawzi, A., Zhou, Q., Shung, K.K., Puliafito, C.A., & Zhang, H.F. Photoacoustic ophthalmoscopy for *in vivo* retinal imaging. *Opt. Express.* **18** (4), 3967-3972 (2010).
7. Wei, Q., Liu, T., Jiao, S., & Zhang, H.F. Image chorioretinal vasculature in albino rats using photoacoustic ophthalmoscopy. *J. Mod. Optic.* **58** (21), 1997-2001, doi:10.1080/09500340.2011.601331 (2011).
8. Liu, T., Wei, Q., Wang, J., Jiao, S., & Zhang, H.F Combined photoacoustic microscopy and optical coherence tomography can measure metabolic rate of oxygen. *Biomed. Opt. Express.* **2** (5), 1359-1365 (2011).
9. Yu, D. & Cringle, S.J. Oxygen distribution and consumption within the retina in vascularised and avascular retinas and in animal models of retinal disease. *Prog. Retin. Eye Res.* **20** (2), 175-208 (2001).
10. Song, W., Wei, Q., Liu, T., Kuai, D., Burke, J.M., Jiao, S., & Zhang, H.F. Integrating photoacoustic ophthalmoscopy with scanning laser ophthalmoscopy, optical coherence tomography, and fluorescein angiography for a multimodal retinal imaging platform. *J. Biomed. Opt.* **17** (6), 061206 (2012).
11. Mark E. Brezinski *Optical Coherence Tomography: Principles and Applications.*, Academic Press, (2006).
12. Hu, S., Rao, B., Maslov, K., & Wang, L.V Label-free photoacoustic ophthalmic angiography. *Opt. Lett.* **35** (1), 1-3 (2010).
13. Zhang, H.F., Maslov, K., & Wang, L.V. *In vivo* imaging of subcutaneous structures using functional photoacoustic microscopy. *Nature protocols.* **2**, 797-804 (2007).
14. Ling, T., Chen, S.L., & Guo, L.J. High-sensitivity and wide-directivity ultrasound detection using high Q polymer microring resonators. *Appl. Phys. Lett.* **98** (20), 204103 (2011).
15. Xie, Z., Jiao, S., Zhang, H.F., & Puliafito, C.A. Laser-scanning optical-resolution photoacoustic microscopy. *Opt. Lett.* **34**, 1771-1773 (2009).

